Dynamic control of light scattering using spatial coherence

Yangyundou Wang,[1] Shenggang Yan,[1] David Kuebel,[2,3] and Taco D. Visser[1,4,5,*]
[1]*ECE/SEI, Northwestern Polytechnical University, 710072 Xi'an, China*
[2]*University of Rochester, Rochester, New York 14627, USA*
[3]*St. John Fisher College, Rochester, New York 14618, USA*
[4]*Department of Physics and Astronomy, VU University, 1081 HV Amsterdam, The Netherlands*
[5]*EEMCS, Delft University of Technology, 2628 CD Delft, The Netherlands*
(Received 21 March 2015; published 6 July 2015)

The scattering of light is perhaps the most fundamental of optical processes. However, active and dynamic control of the directionality of a scattered light field has until now remained elusive. Here we show that with an easily generated, Bessel-correlated field, this goal can be achieved, at least partially. In particular, the angular distribution of a field scattered by a random spherical particle can be tuned to gradually suppress the forward scattering intensity and even create a conelike scattered field. Our method provides a tool for the dynamic control of scattering patterns, both macroscopically and microscopically.

DOI: 10.1103/PhysRevA.92.013806 PACS number(s): 42.25.Fx, 42.25.Kb, 46.65.+g

I. INTRODUCTION

The scattering of wave fields is a process that is encountered in many branches of science, such as astronomy, atmospheric studies, solid state physics, and optics. Because of both its fundamental importance and its many applications, it is highly desirable to achieve active control over the strength and directionality of the scattered field. When a wave is incident on a spherical object, typically a substantial portion of the field is scattered in the forward and in the backward directions. Examples of strong forward scattering are the Mie effect [1, Sec. 14.5], and the Arago-Poisson spot [2, Sec. 8.1]. Kerker *et al.* [3] seem to have been the first to examine under what conditions this angular distribution of the scattered field is modified. Ever since their work, many researchers have analyzed how the composition or geometry of a particle can be chosen such that the scattering in certain directions is suppressed; see, e.g., [4–11]. Here we demonstrate a completely different approach to control the scattering process. By using a scalar field model and applying the first-order Born approximation, we show that dynamic manipulation of the source that generates the incident field, rather than of the scattering object, offers a simple tool to control the angular distribution of the scattered field.

Over the years, many studies have been dedicated to the effects of spatial coherence on the scattering process [12–20]. One typically finds that the scattering remains predominantly in the forward direction, but becomes more diffuse when the spatial coherence of the incident field decreases. However, these studies were limited to Gaussian-correlated fields. Here we report the result that Bessel-correlated fields, which can readily be generated as reported in [21], allow one to dynamically vary the scattering amplitude, making it possible to gradually suppress scattering in the forward direction, and eventually even create a conelike scattered field. We examine scalar fields that are generated by partially coherent, planar sources, and use the first-order Born approximation to study the scattered field that arises when a Gaussian-correlated sphere is placed in the far zone. We compare so-called Gaussian Schell-model sources and uncorrelated annular sources that produce Bessel-correlated fields.

II. PARTIALLY COHERENT SOURCES

Let us consider a secondary, partially coherent, planar source that is situated in the plane $z = 0$, as shown in Fig. 1. The symbol $\boldsymbol{\rho} = (x, y)$ denotes a transverse vector. The coherence properties of the source field at two points $\boldsymbol{\rho}_1$, and $\boldsymbol{\rho}_2$ at frequency ω can be characterized by the cross-spectral-density function [22, Sec. 4.3.2]

$$W^{(0)}(\boldsymbol{\rho}_1, \boldsymbol{\rho}_2, \omega) = \langle U^{(0)*}(\boldsymbol{\rho}_1, \omega) U^{(0)}(\boldsymbol{\rho}_2, \omega) \rangle, \tag{1}$$

where the angular brackets indicate the average taken over an ensemble of realizations of source fields $U^{(0)}(\boldsymbol{\rho}, \omega)$. The cross-spectral density in the far zone of the source, denoted by $W^{(\infty)}$, is given by the formula [22, Eq. 5.3-4]

$$\begin{aligned} &W^{(\infty)}(r_1\mathbf{u}_1, r_2\mathbf{u}_2, \omega) \\ &\quad = \left(\frac{k}{2\pi}\right)^2 \frac{\exp[ik(r_2 - r_1)]}{r_1 r_2} \cos\alpha_1 \cos\alpha_2 \\ &\qquad \times \iint_{z=0} W^{(0)}(\boldsymbol{\rho}_1, \boldsymbol{\rho}_2, \omega) \\ &\qquad \times \exp[-ik(\mathbf{u}_{2\perp} \cdot \boldsymbol{\rho}_2 - \mathbf{u}_{1\perp} \cdot \boldsymbol{\rho}_1)]\, d^2\rho_1 d^2\rho_2, \end{aligned} \tag{2}$$

where $\mathbf{u}_{1\perp}$ and $\mathbf{u}_{2\perp}$ are the projections, considered as two-dimensional vectors, of the three-dimensional directional unit vectors $\mathbf{u}_1$ and $\mathbf{u}_2$ onto the source plane. α_1 and α_2 denote the angles which the vectors $\mathbf{u}_1$ and $\mathbf{u}_2$ make with the positive z axis. A sphere with volume D is located in the far zone of the source, at a distance Δz. If the linear dimensions of the scatterer are assumed to be small compared to Δz, then the angle subtended at the origin O by the scatterer is small, and $\cos\alpha_1 \approx \cos\alpha_2 \approx 1$. Furthermore, the factor $k(r_2 - r_1)$ where $r_i = |(\boldsymbol{\rho}_i, z_i)|$, with $i = 1$ or 2, can then be expressed as

$$k(r_2 - r_1) \approx k\left[z_2\left(1 + \rho_2^2/2z_2^2\right) - z_1\left(1 + \rho_1^2/2z_1^2\right)\right] \tag{3}$$

$$\approx k(z_2 - z_1), \tag{4}$$

*tvisser@nat.vu.nl

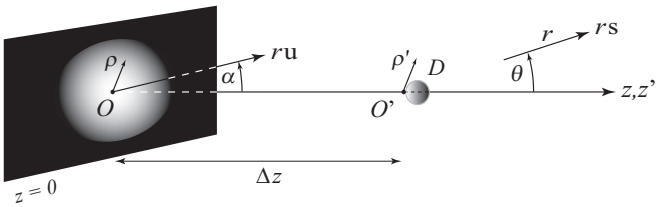

FIG. 1. A secondary, partially coherent source is situated in the plane $z = 0$. A sphere occupying a domain D is located in the far zone, at a distance Δz. The directional unit vector $\mathbf{u}$ and the position z are defined with respect to the origin $O = (0,0,0)$. The directional unit vector $\mathbf{s}$ and the position z' are defined with respect to a second origin $O' = (0,0,\Delta z)$. The transverse vectors $\boldsymbol{\rho} = (x,y)$ and $\boldsymbol{\rho}' = (x',y')$ denote two-dimensional positions.

where we have used the fact that ρ_1 and ρ_2 are both bounded by the transverse size of the scatterer. In addition, the small size of the scatterer implies that the factor $1/r_1 r_2$ does not vary appreciably over its domain D, i.e., $1/r_1 r_2 \approx 1/(\Delta z)^2$. On making use of these approximations in Eq. (2) we obtain the expression

$$W^{(\infty)}(r_1\mathbf{u}_1, r_2\mathbf{u}_2, \omega) = \left(\frac{k}{2\pi\,\Delta z}\right)^2 \exp[ik(z_2 - z_1)] \iint_{z=0} W^{(0)}(\boldsymbol{\rho}_1, \boldsymbol{\rho}_2, \omega) \times \exp[-ik(\mathbf{u}_{2\perp}\cdot\boldsymbol{\rho}_2 - \mathbf{u}_{1\perp}\cdot\boldsymbol{\rho}_1)] d^2\rho_1 d^2\rho_2. \quad (5)$$

It is worth noting that the factor $\exp[ik(z_2 - z_1)]$ implies that the far-zone field is longitudinally fully coherent [22, Sec. 5.2.1]. Before we can use Eq. (5) as an expression for the cross-spectral density of the field that is incident on the scatterer, it must be expressed in terms of the primed variables defined in Fig. 1. This is done by noting that

$$\mathbf{r}_i = r_i\mathbf{u}_i = (\boldsymbol{\rho}_i, z_i) = (\boldsymbol{\rho}_i', z_i), \quad i = 1,2, \quad (6)$$

and hence

$$\mathbf{u}_{i\perp} = \boldsymbol{\rho}_i'/r_i \approx \boldsymbol{\rho}_i'/\Delta z. \quad (7)$$

This allows us to rewrite Eq. (5) as

$$W^{(\mathrm{inc})}(\mathbf{r}_1', \mathbf{r}_2', \omega) = \left(\frac{k}{2\pi\,\Delta z}\right)^2 \exp[ik(z_2' - z_1')] \times \iint_{z=0} W^{(0)}(\boldsymbol{\rho}_1, \boldsymbol{\rho}_2, \omega) \times \exp[-ik(\boldsymbol{\rho}_2'\cdot\boldsymbol{\rho}_2 - \boldsymbol{\rho}_1'\cdot\boldsymbol{\rho}_1)/\Delta z]\, d^2\rho_1 d^2\rho_2, \quad (8)$$

where the superscript "inc" indicates the incident field. We will make use of Eq. (8) to determine the cross-spectral density of the field incident on the scattering volume D for different kinds of sources.

III. SCATTERING BY A GAUSSIAN-CORRELATED SPHERE

Suppose first that a deterministic field $U^{(\mathrm{inc})}(\mathbf{r},\omega)$ is incident on a deterministic scatterer. The space-dependent part of the scattered field $U^{(\mathrm{sca})}(\mathbf{r},\omega)$ is, within the accuracy of the first-order Born approximation, given by the expression [1, Sec. 13.1.2]

$$U^{(\mathrm{sca})}(\mathbf{r},\omega) = \int_D F(\mathbf{r}',\omega) U^{(\mathrm{inc})}(\mathbf{r}',\omega) G(\mathbf{r},\mathbf{r}',\omega)\, d^3r', \quad (9)$$

where

$$F(\mathbf{r},\omega) = \frac{k^2}{4\pi}[n^2(\mathbf{r},\omega) - 1] \quad (10)$$

denotes the scattering potential of the medium, $n(\mathbf{r},\omega)$ being its refractive index, and

$$G(\mathbf{r},\mathbf{r}',\omega) = \frac{\exp(ik|\mathbf{r} - \mathbf{r}'|)}{|\mathbf{r} - \mathbf{r}'|} \quad (11)$$

is the outgoing free-space Green's function of the Helmholtz operator.

We choose the origin O' of a second Cartesian coordinate system at the front face of the scatterer and consider the field at a point $\mathbf{r}$ in its far zone, as sketched in Fig. 1. Setting $\mathbf{r} = r\mathbf{s}$, with $\mathbf{s}$ a unit directional vector, the Green's function in the far zone may be approximated by the expression

$$G(\mathbf{r},\mathbf{r}',\omega) \sim \frac{\exp(ikr)}{r} \exp(-ik\mathbf{s}\cdot\mathbf{r}'). \quad (12)$$

For a random scatterer the scattering potential is a random function of position. Let

$$C_F(\mathbf{r}_1', \mathbf{r}_2', \omega) = \langle F^*(\mathbf{r}_1', \omega) F(\mathbf{r}_2', \omega)\rangle_F \quad (13)$$

be its correlation function. The angular brackets denote the average, taken over an ensemble of realizations of the scattering potential. We will consider scattering from a Gaussian-correlated, homogeneous, isotropic sphere. Then

$$C_F(\mathbf{r}_1', \mathbf{r}_2', \omega) = C_0 \exp\big[-(\mathbf{r}_2' - \mathbf{r}_1')^2/2\sigma_F^2\big], \quad (14)$$

where C_0 is a positive constant, and the coherence length σ_F is assumed to be small compared with the linear dimensions of the scattering volume. This assumption will later allow us to extend the domain of integration to $\mathbb{R}^3$. Next we assume that the incident field is partially coherent. Because of the random nature of both the incident field and the scatterer, the scattered field will, of course, also be random. Its cross-spectral-density function is defined, in complete analogy with Eq. (1), as

$$W^{(\mathrm{sca})}(\mathbf{r}_1, \mathbf{r}_2, \omega) = \langle U^{(\mathrm{sca})^*}(\mathbf{r}_1, \omega) U^{(\mathrm{sca})}(\mathbf{r}_2, \omega)\rangle, \quad (15)$$

where the angular brackets indicate the average taken over an ensemble of realizations of the scattered field. On substituting from Eqs. (9) and (13) into Eq. (15) and interchanging the order of integration and ensemble averaging, we find the formula

$$W^{(\mathrm{sca})}(\mathbf{r}_1, \mathbf{r}_2, \omega) = \iint_D W^{(\mathrm{inc})}(\mathbf{r}_1', \mathbf{r}_2', \omega) C_F(\mathbf{r}_1', \mathbf{r}_2', \omega) \times G^*(\mathbf{r}_1, \mathbf{r}_1', \omega) G(\mathbf{r}_2, \mathbf{r}_2', \omega)\, d^3r_1' d^3r_2'. \quad (16)$$

The spectral density of the scattered field, $S^{(\mathrm{sca})}(\mathbf{r},\omega)$, is obtained by setting the two positions $\mathbf{r}_1$ and $\mathbf{r}_2$ equal,

i.e.,

$$S^{(\mathrm{sca})}(\mathbf{r},\omega) = W^{(\mathrm{sca})}(\mathbf{r},\mathbf{r},\omega), \tag{17}$$

$$= \frac{C_0}{r^2}\iint_D W^{(\mathrm{inc})}(\mathbf{r}_1',\mathbf{r}_2',\omega)\exp\left[-(\mathbf{r}_2'-\mathbf{r}_1')^2/2\sigma_F^2\right] \times \exp[-ik\mathbf{s}\cdot(\mathbf{r}_2'-\mathbf{r}_1')]\,d^3r_1'd^3r_2', \tag{18}$$

where we have used Eqs. (12) and (14). Before proceeding, we note that Eq. (18) relates the cross-spectral density of the incident field, $W^{(\mathrm{inc})}$, with the distribution of the scattered field in the far zone, $S^{(\mathrm{sca})}$. This relation has the form of a Fourier transform of the cross-spectral density, weighed with a Gaussian factor. In view of Eq. (8), which is also a Fourier transform, one might then suspect, on the basis of the van Cittert–Zernike theorem [22, Sec. 4.4.4], that the shape of a δ-correlated source is somehow mimicked by the scattered field. This observation was the motivation for this study.

Next we will analyze the consequences of Eq. (18) for incident fields generated by sources with different coherence properties. To simplify the notation we suppress the ω dependence of the various quantities from now on.

IV. GAUSSIAN SCHELL-MODEL SOURCES

Let us first assume that the source is of the Gaussian Schell-model type. Such sources have a cross-spectral density of the form [23, Sec. 5.3.1]

$$W^{(0)}(\boldsymbol{\rho}_1,\boldsymbol{\rho}_2) = [S^{(0)}(\boldsymbol{\rho}_1)]^{1/2}[S^{(0)}(\boldsymbol{\rho}_2)]^{1/2}\mu^{(0)}(\boldsymbol{\rho}_1-\boldsymbol{\rho}_2,), \tag{19}$$

with

$$S^{(0)}(\boldsymbol{\rho}) = A^2\exp\left(-\rho^2/2\sigma_S^2\right), \tag{20}$$

$$\mu^{(0)}(\boldsymbol{\rho}_1-\boldsymbol{\rho}_2) = \exp\left[-(\boldsymbol{\rho}_2-\boldsymbol{\rho}_1)^2/2\sigma_\mu^2\right], \tag{21}$$

representing the spectral density and the spectral degree of coherence of the source field, respectively, the constants A, σ_S, and σ_μ being positive quantities. On substituting from Eqs. (19)–(21) into Eq. (8) we obtain the formula

$$W^{(\mathrm{inc})}(\mathbf{r}_1',\mathbf{r}_2') = \left(\frac{kA\sigma_S\sigma_{\mathrm{eff}}}{\Delta z}\right)^2\exp[ik(z_2'-z_1')] \times \exp\left[\frac{-k^2\sigma_S^2(\boldsymbol{\rho}_2'-\boldsymbol{\rho}_1')^2}{2(\Delta z)^2}\right] \times \exp\left[\frac{-k^2\sigma_{\mathrm{eff}}^2(\boldsymbol{\rho}_2'+\boldsymbol{\rho}_1')^2}{8(\Delta z)^2}\right], \tag{22}$$

where

$$\frac{1}{\sigma_{\mathrm{eff}}^2} = \frac{1}{4\sigma_S^2} + \frac{1}{\sigma_\mu^2}. \tag{23}$$

On making use of Eq. (22) in expression (18), we find that the normalized distribution of the scattered intensity is given by the expression

$$S_N^{(\mathrm{sca})}(\theta) = S^{(\mathrm{sca})}(\theta)/S^{(\mathrm{sca})}(\theta=0) \tag{24}$$

$$= \exp[-k^2\sigma_F^2(1-|,\cos\theta)^2/2]\exp[-k^2\sin^2\theta/4\Gamma], \tag{25}$$

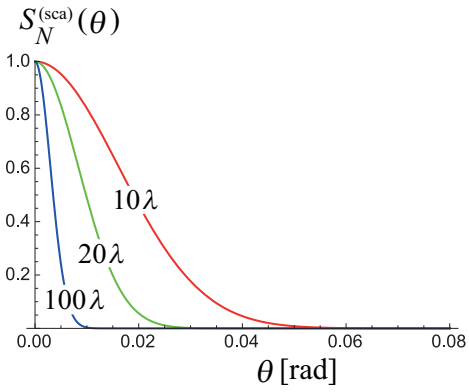

FIG. 2. (Color online) The normalized spectral density of the scattered field for selected values of the effective correlation length of the sphere: $\sigma_F = 10\lambda$ (red), 20λ (green), and 100λ (blue). In these examples the wavelength $\lambda = 0.6328$ μm, $\sigma_S = 1$ cm, and $\Delta z = 4$ m.

where

$$\Gamma = \frac{k^2\sigma_S^2}{2\Delta z^2} + \frac{1}{2\sigma_F^2}, \tag{26}$$

and θ denotes the scattering angle, shown in Fig. 1. It is seen from Eq. (25) that the scattered field depends on the two length scales σ_S and σ_F. Notice that there is no dependence on the correlation length σ_μ of the source. This is a consequence of the fact that the scattering volume is located in the far zone, which means that the field in the vicinity of the z' axis has become essentially transversely coherent, as is discussed in [22, Sec. 5.6.4]. In Fig. 2 the spectral density of the scattered field is shown for different values of σ_F, the effective correlation length of the scatterer. It is seen that the scattering becomes more directional when σ_F increases. However, in all cases the scattering reaches its maximum value in the forward direction ($\theta = 0$). The scattered intensity for angles larger than 0.08 is negligible.

V. UNCORRELATED ANNULAR SOURCES

Next we consider a completely incoherent (i.e., δ correlated), ring-shaped source with a uniform spectral density, and with inner radius a and outer radius b. The realization of such a source was reported in [21]. In this case the spectral density and the spectral degree of coherence in the source plane are

$$S^{(0)}(\boldsymbol{\rho}) = A^2[\mathrm{circ}(\rho/b) - \mathrm{circ}(\rho/a)], \tag{27}$$

$$\mu^{(0)}(\boldsymbol{\rho}_1,\boldsymbol{\rho}_2) = \delta^2(\boldsymbol{\rho}_2-\boldsymbol{\rho}_1), \tag{28}$$

where δ^2 denotes the two-dimensional Dirac δ function, and $\mathrm{circ}(x)$ the circle function; $\mathrm{circ}(x) = 1$ if $x \leqslant 1$, and 0 otherwise. Hence

$$W^{(0)}(\boldsymbol{\rho}_1,\boldsymbol{\rho}_2) = A^2[\mathrm{circ}(\rho_1/b) - \mathrm{circ}(\rho_1/a)]^{1/2} \times [\mathrm{circ}(\rho_2/b) - \mathrm{circ}(\rho_2/a)]^{1/2}\delta^2(\boldsymbol{\rho}_2-\boldsymbol{\rho}_1). \tag{29}$$

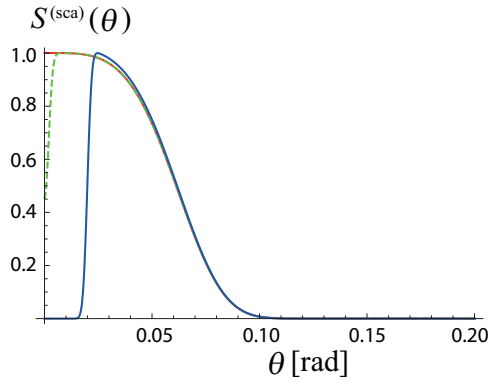

FIG. 3. (Color online) Angular distribution of the scattered field for various choices of the inner radius a of an annular source: $a = 0$ (red), 2 mm (dashed green), and 2 cm (blue). The curves are normalized to unity. In this example $\lambda = 0.6328\ \mu$m, $\Delta z = 1$ m, $\sigma_F = 100\lambda$, and the outer radius $b = 15$ cm.

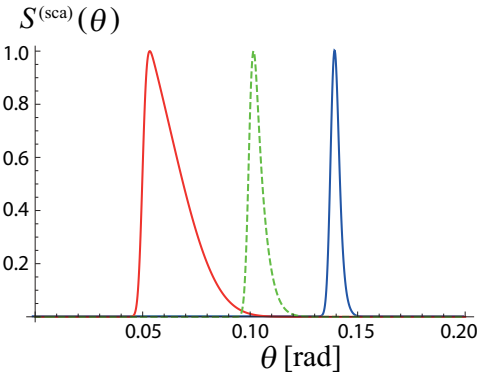

FIG. 4. (Color online) Angular distribution of the scattered field for various choices of the inner radius a of an annular source: $a =$ 5 cm (red), 10 cm (dashed green), and 14 cm (blue). The curves are normalized to unity. The parameters are the same as in Fig. 3.

On substituting from this formula into Eq. (8) we find that

$$W^{(\mathrm{inc})}(\mathbf{r}_1', \mathbf{r}_2') = \frac{kA^2}{2\pi\Delta z}\exp[ik(z_2' - z_1')] \times\left[\frac{bJ_1(kb|\boldsymbol{\rho}_2' - \boldsymbol{\rho}_1'|/\Delta z)}{|\boldsymbol{\rho}_2' - \boldsymbol{\rho}_1'|} - \frac{aJ_1\left(ka|\boldsymbol{\rho}_2' - \boldsymbol{\rho}_1'|/\Delta z\right)}{|\boldsymbol{\rho}_2' - \boldsymbol{\rho}_1'|}\right], \tag{30}$$

where J_1 denotes the Bessel function of the first kind of order 1. On using Eq. (30) in Eq. (18) we obtain for the scattered intensity the expression

$$S^{(\mathrm{sca})}(\theta) = C\exp\left[-\frac{k^2\sigma_F^2(1-\cos\theta)^2}{2}\right] \times\int_0^\infty\left[bJ_1\left(\frac{kb\rho}{\Delta z}\right) - aJ_1\left(\frac{ka\rho}{\Delta z}\right)\right] \times J_0(k\rho\sin\theta)\exp\left(-\frac{\rho^2}{2\sigma_F^2}\right)d\rho. \tag{31}$$

where C is a constant, independent of the angle θ. The results of a numerical evaluation of Eq. (31) are shown in Fig. 3. When the inner radius $a = 0$, meaning that the source is circular, the scattered field has a broad distribution that is centered on the forward direction $\theta = 0$. When $a = 2$ mm, the forward scattered field has a decreased intensity that is only 45% of the maximum value, which occurs near $\theta = 0.01$. Increasing the inner radius a to 2 cm produces a scattered field that is essentially zero in the forward direction and reaches a peak near $\theta = 0.025$. The effects of further increasing the inner radius a are illustrated in Fig. 4. The scattered field distribution becomes gradually narrower, and the direction of maximum intensity increases, eventually reaching a value of 8°. This conelike scattering that is obtained with a Bessel-correlated field is in marked contrast with the diffuse forward scattering that arises from a Gaussian-correlated field, as was shown in Fig. 2.

It is to be noted that, although we have presented examples at optical frequencies and scatterers with dimensions of $\sim 100\lambda$, we expect this method to work equally well at longer wavelengths and for larger objects.

Finally, the question of how zero forward scattering can be compatible with the optical theorem was raised several years ago [4]. Since this theorem holds only for deterministic scatterers that are illuminated by a fully coherent, monochromatic plane wave [24], and because these two conditions are not satisfied here, it clearly does not apply to the present case.

VI. CONCLUSIONS

We have demonstrated how the angular distribution of a field that is scattered by a random, Gaussian-correlated sphere can be manipulated using spatial coherence. Two types of sources were examined: Gaussian Schell-model sources and incoherent annular sources. The first produces a Gaussian-correlated field, the second a Bessel-correlated field. Using the first-order Born approximation, it was found that a Gaussian-correlated field gives rise to scattering that is predominantly in the forward direction. In stark contrast, the Bessel-correlated field was shown to lead to a decreased forward scattering. By simply varying the size of an uncorrelated annular source, the scattering distribution can be tuned, and can even take on a conelike form without any forward scattering. Unlike the use of specially designed scatterers which produce a single, static field distribution, our approach can be used to dynamically alter the scattered field. We believe that our approach offers a further tool among the many uses of light scattering [25]. For example, this method may be used to selectively address detectors that are positioned at different angles, or in cloaking [26].

[1] M. Born and E. Wolf, *Principles of Optics* (Cambridge University Press, Cambridge, 1995).

[2] H. C. van de Hulst, *Light Scattering from Small Particles* (Dover, New York, 1981).

[3] M. Kerker, D.-S. Wang, and C. L. Giles, J. Opt. Soc. Am. **73**, 765 (1983).
[4] A. Alu and N. Engheta, J. Nanophotonics **4**, 041590 (2010).
[5] M. Nieto-Vesperinas, R. Gomez-Medina, and J. J. Saenz, J. Opt. Soc. Am. A **28**, 54 (2011).
[6] B. Garcia-Camara *et al.*, Opt. Lett. **36**, 728 (2011).
[7] J. M. Geffrin *et al.*, Nat. Commun. **3**, 1171 (2012).
[8] S. Person, M. Jain, Z. Lapin, J. J. Saenz, G. Wicks, and L. Novotny, Nano Lett. **13**, 1806 (2013).
[9] Y.-M. Xie, W. Tan, and Z.-G. Wang, Opt. Express **23**, 2091 (2015).
[10] O. Korotkova, Opt. Lett. **40**, 284 (2015).
[11] R. R. Naraghi, S. Sukhov, and A. Dogariu, Opt. Lett. **40**, 585 (2015).
[12] W. H. Carter and E. Wolf, Opt. Commun. **67**, 85 (1988).
[13] J. Jannson, T. Jannson, and E. Wolf, Opt. Lett. **13**, 1060 (1988).
[14] F. Gori, C. Palma, and M. Santarsiero, Opt. Commun. **74**, 353 (1990).
[15] P. S. Carney and E. Wolf, Opt. Commun. **155**, 1 (1998).
[16] D. Cabaret, S. Rossano, and C. Brouder, Opt. Commun. **150**, 239 (1998).
[17] T. D. Visser, D. G. Fischer, and E. Wolf, J. Opt. Soc. Am. A **23**, 1631 (2006).
[18] J.-J. Greffet, M. De La Cruz-Gutierrez, P. V. Ignatovich, and A. Radunsky, J. Opt. Soc. Am. A **20**, 2315 (2003).
[19] T. van Dijk, D. G. Fischer, T. D. Visser, and E. Wolf, Phys. Rev. Lett. **104**, 173902 (2010).
[20] D. G. Fischer, T. van Dijk, T. D. Visser, and E. Wolf, J. Opt. Soc. Am. A **29**, 78 (2012).
[21] S. B. Raghunathan, T. van Dijk, E. J. G. Peterman, and T. D. Visser, Opt. Lett. **35**, 4166 (2010).
[22] L. Mandel and E. Wolf, *Optical Coherence and Quantum Optics* (Cambridge University Press, Cambridge, 1995).
[23] E. Wolf, *Introduction to the Theory of Coherence and Polarization of Light* (Cambridge University Press, Cambridge, 2007).
[24] P. S. Carney, E. Wolf, and G. S. Agarwal, J. Opt. Soc. Am. A **14**, 3366 (1997).
[25] *The Mie Theory—Basics and Applications*, edited by W. Hergert and T. Wriedt (Springer, Heidelberg, 2012).
[26] A. Alu and N. Engheta, Phys. Rev. Lett. **102**, 233901 (2009).